



## Adsorption characteristic of organic matter by low-temperature dry cattle manure-derived anaerobic digestion

Yao Zhu<sup>a,c</sup>, Baojun Yi<sup>a,b,\*</sup>, Zhixi Zong<sup>a</sup>, Xueqi Yang<sup>a</sup>, Meijing Chen<sup>a</sup>, Qiaoxia Yuan<sup>a,b</sup>

<sup>a</sup>College of Engineering, Huazhong Agricultural University, No. 1, Shizishan Street, Hongshan District, Wuhan 430070, China, Tel./Fax: +86 27 87282120; emails: bjyi@mail.hzau.edu.cn (B. Yi), 2015307201530@webmail.hzau.edu.cn (Y. Zhu), zongzhixi@webmail.hzau.edu.cn (Z. Zong), yangxueqi@webmail.hzau.edu.cn (X. Yang), 2017307220432@webmail.hzau.edu.cn (M. Chen), qxyuan@mai.hzau.edu.cn (Q. Yuan)

<sup>b</sup>Key Laboratory of Agricultural Equipment in the Mid-lower Yangtze River, Ministry of Agriculture, Wuhan 430070, China

<sup>c</sup>State Key Laboratory of Clean Energy Utilization, Institute for Thermal Power Engineering, Zhejiang University, Hangzhou 310027, China

Received 4 May 2020; Accepted 18 February 2021

### ABSTRACT

Anaerobic digestion (AD) prepared with the biogas industry can be utilised to adsorb organic matter in wastewater for realising the resource utilisation of AD. The low-temperature dry cattle manure-derived anaerobic digestion (CMAD) is a potential method for preparing adsorbents. Slow pyrolytic carbon (CMSP) and fast pyrolytic carbon (CMFP) are prepared to compare the adsorption capacity of CMAD. This study conducts the characteristic tests, adsorption experiments and isotherm and kinetics analyses of these samples. Results show that the surface functional groups of CMAD are abundant, and the surface area is small. The adsorptions of Methylene blue (MB) on CMSP, CMFP and CMAD reach a slow adsorption process at 240, 360 and 120 min, respectively. The maximum removal amounts by CMSP, CMFP and CMAD are 96.88%, 53.03% and 95.72% for MB. The adsorption of MB and Congo red (CR) by CMAD appears as a heterogeneous monolayer on the basis of adsorption isotherm and kinetics. The adsorptions of MB and CR by CMAD are chemical and physical adsorptions, respectively. CMAD can be utilised as an adsorbent due to its rich functional groups. In the meantime, its adsorption performance can be largely enhanced by improving its specific surface area.

*Keywords:* Cattle manure; Anaerobic digestion; Adsorption characteristic; Methylene blue; Congo red

### 1. Introduction

The reproducibility and biodegradability of biomass resources, as the exhaustion of fossil energy, have attracted increasing attention. Biochemistry and thermochemistry are widely used in biomass energy conversion, but the former is more economical than the latter [1].

Anaerobic fermentation is an important method for the biochemical technology of biomass and a primary method to reduce organic waste [2]. Large amounts of

anaerobic digestion (AD) are produced with the development of the biogas industry [3,4]. AD contains mineral nitrogen ( $\text{NH}_4^+\text{-N}$ ), a large number of elements (N, P, K, Ca and Mg), trace elements (Fe, Al, Cu and Zn) and organic substances necessary for plant growth; thus, it is generally utilised as a soil fertiliser [3]. However, AD utilised as fertiliser has exceeded the affordability of nearby farmland [5].

The preparation of biochar from AD can expand the application range of AD [6]. Straw AD is more suitable for carbon production given that straw has a rich cellulose component. Straw AD biochar with excellent performance

\* Corresponding author.

is mainly applied to remove heavy metals from wastewater because of the loose porosity and high stability [5,7,8]. By contrast, the AD from livestock manure is generally considered unsuitable for the preparation of biochar due to the high contents of organic matter and minerals [5]. However, our previous study showed that biochar from cattle manure is a good adsorbent because of the rich mineral content [9]. Previous research shows that the mineral component has excellent adsorption properties for heavy metal in solution [10], even though it has a small specific surface area and high ash content. Livestock wastewater contains a high concentration of chemical oxygen demand, which is mainly composed of organic matter. Thus, livestock manure AD after drying can be used to adsorb organic matter. In our previous research, the organic matter can be effectively removed by low-temperature pyrolysis of livestock manure.

In the present study, Congo red (CR) and Methylene blue (MB) are selected as the representatives of acidic and alkaline organic compounds [11,12]. The physicochemical properties and adsorption characteristics of low-temperature dry cattle manure-derived anaerobic digestion (CMAD) are analysed. It is compared with two typical types of pyrolysis carbon prepared from cattle manure (with properties closer to activated carbon) to study the potential of the CMAD as an adsorbent. Whether CMAD can have excellent adsorption performance without a high-temperature treatment is also explored. An environmentally friendly AD treatment method is investigated to provide a basis for AD recycling.

## 2. Materials and method

### 2.1. Materials and reagents

AD samples were taken from the biogas tank of the Laboratory of Huazhong Agricultural University. Firstly, low-temperature dry cattle manure-derived AD was dried, and the impurities were filtered by a sieve. Then, the sample was crushed with a mortar. It was then screened through a 60–200 mesh sieve and placed in a 45°C until the weight change did not exceed 0.1% every 2 h, and this sample was recorded as CMAD and bagged for preservation. Fresh cattle manure was collected from a farm in Wuhan (Wuhan, China). Fresh cattle manure was dried, bagged and stored in the refrigerator. The fresh cattle manure was dried in a 105°C oven for 24 h and then sieved through a 60–200 mesh sieve to uniform particle size, and this sample was named CM. The preparation method of slow pyrolysis carbon was as follows. Before the experiment, N<sub>2</sub> gas was introduced into the muffle furnace to ensure an oxygen-deficient environment. A total of 30 g of CM was placed in a porcelain boat, which was then placed in a muffle furnace. The furnace temperature was set to rise from room temperature to 900°C in 30 min and kept for 30 min. The muffle furnace was turned off to cool the biochar to room temperature. The sample was recorded as Slow pyrolytic carbon (CMSP). The difference between fast and slow pyrolysis carbon was that the abovementioned sample was directly placed in a muffle furnace at 900°C for 30 min and then cooled to room temperature. The sample was recorded as fast pyrolytic carbon (CMFP). MB and CR were purchased from Sinopharm (China), and they were used without further purification.

### 2.2. Characterisation methods

The characteristic test is as follows: elemental analysis; scanning electron microscopy; Brunauer–Emmett–Teller test (BET); Fourier transform infrared spectroscopy (FTIR); X-ray diffraction (XRD); Thermogravimetric analysis–derivative thermogravimetry (TG–DTG); zero point charge test (pH<sub>zpc</sub>) [13].

### 2.3. Adsorption experiments

The adsorption performance of CMAD was studied by adsorption experiment and compared with that of CMSP and CMFP. The MB and CR concentrations in solution were analysed using a UV spectrophotometer of UH5300 from Hitachi (Japan), by monitoring the absorbance changes at the wavelengths of 660 and 510 nm, respectively [14]. The calculation formula of adsorption quantity ( $q_t$ , mg g<sup>-1</sup>) and removal rate ( $R$ ) are as follows [15]:

$$q_t = \frac{(C_0 - C_t)V}{W} \quad (1)$$

$$R = \frac{100(C_0 - C_t)}{C_0} \quad (2)$$

where  $C_0$  and  $C_t$  are the concentrations of MB and CR at the initial and  $t$  moments (mg L<sup>-1</sup>), respectively.  $V$  is the solution volume (L), and  $W$  is the absorbed dose (g).

## 3. Results and discussion

### 3.1. Characterisation of samples

The physical and chemical properties of CMAD, CMSP and CMFP are shown in Table 1. The H content of biochar declines due to the pyrolysis of the nitrile group and the heterocyclic compound at high temperature [6]. Thus, the C content of CMAD is significantly lower than that of CMSP and CMFP, whilst the O and H contents are higher than those of CMSP and CMFP.

Given the high C, H, O and N contents and a low ash content of the CMAD, its cellulose, hemicellulose and lignin are higher than those of CMSP and CMFP. The molar ratios of C, H and O can exhibit the relationship between pyrolysis temperature and the aromaticity and hydrophobicity of the material. H/C and O/C ratios are applied to evaluate the degree of carbonisation and surface hydrophilicity, respectively [7,16,17]. The H/C molar ratio of CMAD is 1.44, whilst those of CMSP and CMFP are 0.5 and 0.42, respectively. This finding indicates that the degree of graphitisation of CMAD is low and the organic component is high. Comparing the O/C ratio of CMAD with those of CMSP and CMFP shows that the CMAD is more hydrophilic. The functional groups on the surface of the biochar decompose and decline after pyrolysis. The H and O contents of CMSP and CMFP are less than those of CMAD because of the content of surface functional groups.

The surface morphology characteristics of CMAD, CMSP and CMFP are shown in Fig. 1. Obvious differences are observed amongst CMAD, CMSP and CMFP. The

Table 1  
Physical and chemical properties of samples

Sample	Proximate analysis (wt.%ad)				Ultimate analysis (wt.%daf)						pH <sub>zpc</sub>
	M	VM	FC	A	C	H	O <sup>a</sup>	N	O/C	H/C	
CMAD	4.68	54.10	15.01	26.21	57.53	6.92	33.40	1.85	0.44	1.44	7.41
CMSP	3.40	6.92	24.03	65.65	82.14	3.44	10.53	2.84	0.096	0.50	9.49
CMFP	2.98	5.83	30.44	60.75	87.79	3.08	5.45	2.84	0.046	0.42	10.68

O<sup>a</sup>: calculated by difference.

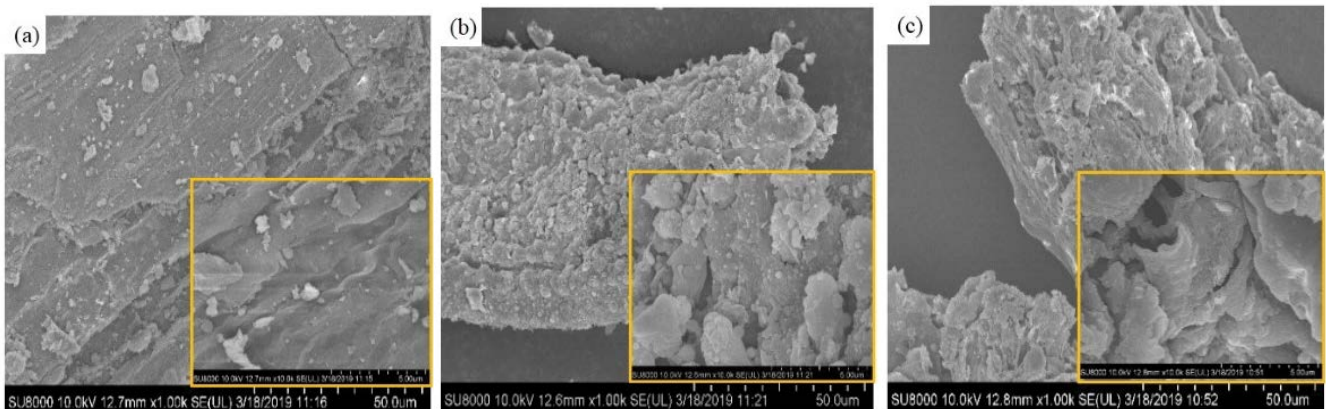


Fig. 1. Surface micrographs of samples: (a) CMAD, (b) CMSP, and (c) CMFP.

surface of CMSP and CMFP has abundant pore structure, whilst that of CMAD is smooth and has no pore structure. Therefore, CMAD has a weak physical adsorption.

The pore structure of CMAD, CMSP and CMFP and N<sub>2</sub> adsorption/desorption isotherm are shown in Fig. 2. The specific surface area of CMSP is the largest up to 163.57 m<sup>2</sup> g<sup>-1</sup>, whilst that of CMAD is very small with 2.14 m<sup>2</sup> g<sup>-1</sup>. Notably,  $d < 2$  nm is micropore,  $2 < d < 50$  nm is mesopore and  $d > 50$  nm is macropore [18]. As shown in Fig. 2b, CMSP has many micropores and mesopores,

CMFP has many mesopores and CMAD has little on the two pores. Micropores and mesopores are the main reasons for the good physical adsorption performance of biochar [19]. Thus, CMSP has the best adsorption capacity in terms of physical adsorption performance.

The pore structure and the properties of surface functional groups affect the adsorption capacity of biochar. The FTIR spectrum of the three samples is shown in Fig. 3. The band at 3,000–3,400 cm<sup>-1</sup> is assigned to –OH [20]. The bands at 2,927 and 2,855 cm<sup>-1</sup> are attributed to the aliphatic

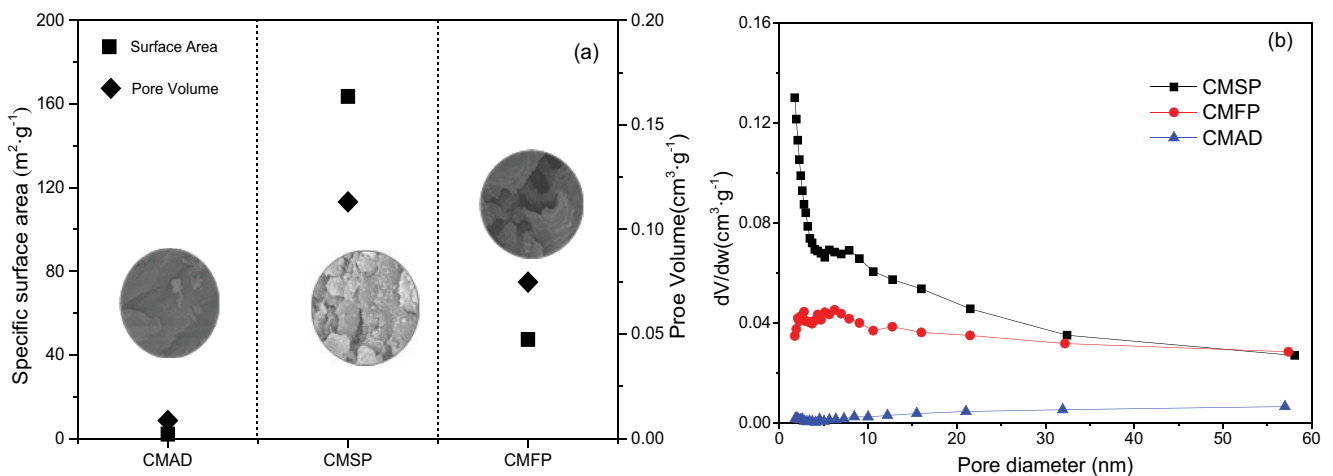


Fig. 2. Pore structure characteristic of samples: (a) specific surface area and total pore volume and (b) distribution of pore volumes in pore diameter.

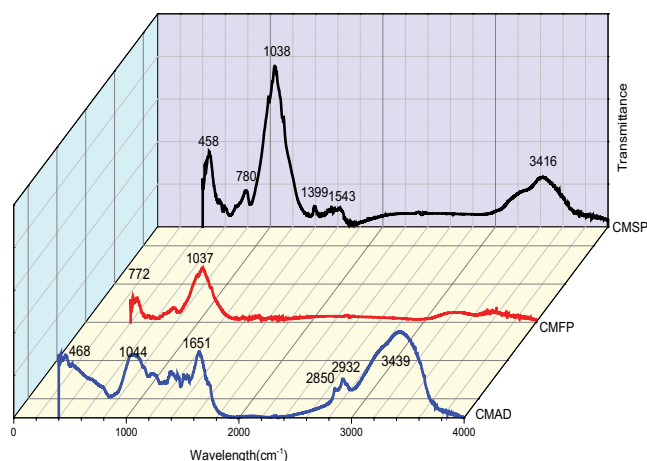


Fig. 3. FTIR spectrum of samples.

C–H groups [7,21]. The band at around  $1,651\text{ cm}^{-1}$  is C=C and C=O groups [22]. Notably,  $1,040\text{ cm}^{-1}$  belongs to the C–O group [23]. The bands at approximately  $400$  and  $780\text{ cm}^{-1}$  correspond to the Si–O stretching vibrations [16], and  $1,420\text{ cm}^{-1}$  belongs to  $\text{CH}_2$  [7]. The hydroxyl groups on the CMAD and CMSP are nearly  $3,418$  and  $3,439\text{ cm}^{-1}$ , respectively, which indicates that the hydroxyl groups change significantly after fermentation and pyrolysis. The decreases in H content in CMSP and CMFP cause the disappearance of the C–H structure. A peak at  $780\text{ cm}^{-1}$  appears on CMSP and CMFP but not on CMAD, which implies that the aromatic hydrocarbon content of CMSP and CMFP is higher than that of CMAD. CMAD surface has a rich number and variety of functional groups, and the structure of the functional groups of CMSP is closer to that of CMAD. A previous study showed that the type and concentration of functional groups play an important role in the adsorption process [17]. Therefore, the great adsorption properties of CMAD are attributed to the chemical adsorption caused by functional groups. In a word, the surface functional groups of the three materials are qualitatively different because of different treatment methods and pyrolysis conditions.

XRD is an important method to analyse the crystallinity of materials. The XRD diffraction patterns of CMAD, CMSP and CMFP are shown in Fig. 4. The interlayer spacing between the monolayers of the aromatic layer ( $d_{002}$ ) and crystallite height of the microcrystalline layer ( $L_c$ ) is calculated [24]. Smaller  $d_{002}$  and  $L_c$  correspond to a more stable crystal structure [25]. Fig. 4 shows that all samples have a 002 diffraction peak. The  $d_{002}$  of graphite is  $0.3354\text{ nm}$  [26]. The  $d_{002}$  of CMAD is larger than those of CMSP and CMFP, which implies that CMSP and CMFP have a high degree of graphitisation and strong stability. The  $L_c$  of CMAD that is nearly twice as much like that of CMSP and CMFP demonstrates that amorphous carbon with low crystallinity exists in CMAD. The degree of CMAD graphitisation is low, and its stability is poor.

The thermal stability of CMAD is analysed by TG–DTG curve in Fig. 5. The weight loss of the first and second parts is related to the removal of free water in biochar and the decomposition of cellulose and hemicellulose, respectively [27,28]. When the pyrolysis temperature is lower

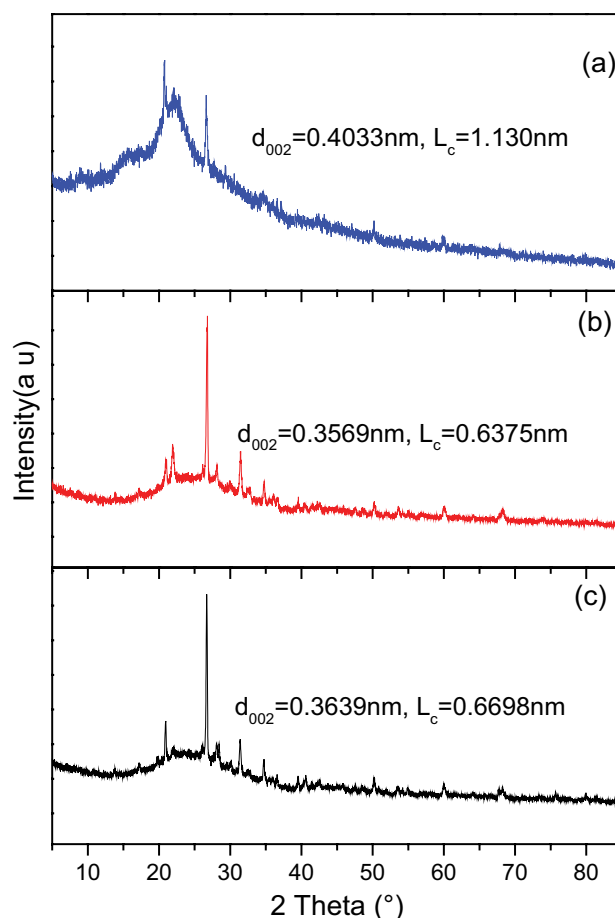


Fig. 4. XRD pattern of samples: (a) CMAD, (b) CMSP, and (c) CMFP.

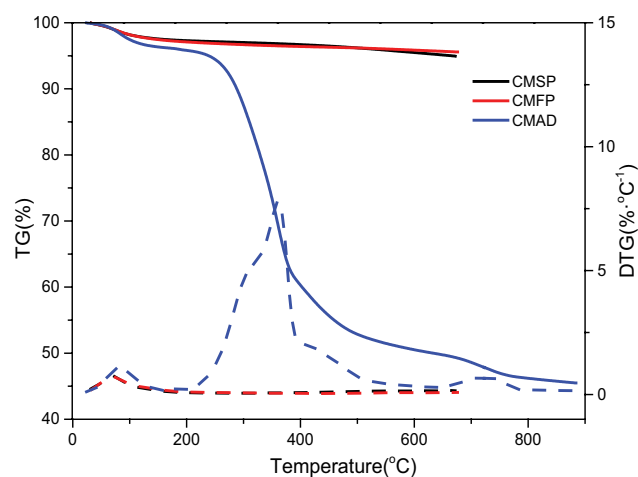


Fig. 5. Thermogravimetric analysis of samples.

than  $100^\circ\text{C}$ , the weight of the three samples drops slightly due to the release of free water. The weight loss of CMAD is approximately 50% in the range of  $200^\circ\text{C}$ – $400^\circ\text{C}$ , which can be attributed to the degradation of hemicellulose and cellulose. The final 45% residual amount indicates that CMAD is rich in volatile substances and organic matter.

In the meantime, the mass loss of CMSP and CMFP is less than 10% after pyrolysis indicating a low volatile matter content and high stability. This finding is consistent with the results of the proximate analysis.

### 3.2. Adsorption characteristics

#### 3.2.1. Comparison of adsorption properties amongst CMAD, CMSP and CMFP

The adsorption experimental results of original matter by CMAD, CMSP and CMFP are shown in Fig. 6 for determining the affecting factors of the adsorption performance of CMAD. Our previous study showed that the adsorption of MB is related to the surface functional groups of biochar [9]. The MB adsorption amount improves with the increase in the H/C molar ratio. The surface functional groups greatly affect the MB adsorption given that the molar ratio of O/C and H/C is proportional to the content of functional groups. In the meantime, surface area affects the adsorption capacity of biochar to CR [29]. Given that the molecular size of CR ( $d$  is approximately 1 nm) is larger than that of MB ( $d$  is nearly 0.7 nm) [18], a relatively large mesopore with a small diffusion resistance against CR is conducive to CR adsorption. The pore diameter test and adsorption experiment show that the adsorption of CR and MB is mainly affected by mesopores and micropores, respectively.

CMAD has good adsorption properties for MB because its surface is rich in functional groups. However, CMAD contains few micropores and mesopores and thus has poor

adsorption performance for CR. Therefore, CMAD can be used as an adsorbent for alkaline organic matter. Its adsorption performance is mainly affected by chemical adsorption related to its surface oxygen-containing functional groups. The physical adsorption of CMAD is very weak and can be ignored.

#### 3.2.2. Effects of solution concentrations and adsorption time on adsorption

The adsorption results at a different time and solution concentrations are shown in Fig. 7. The adsorption amount

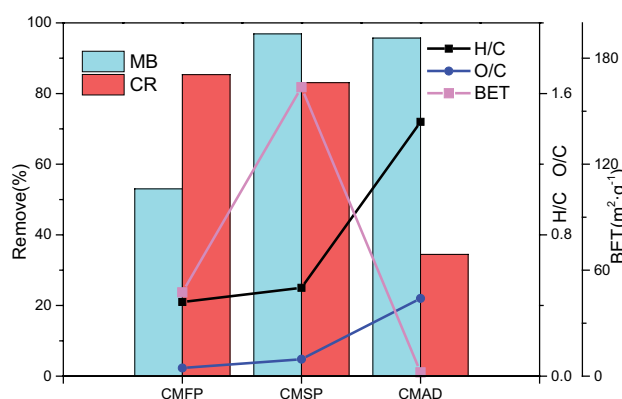


Fig. 6. Effect of characteristic on adsorption of original matter by CMAD, CMSP and CMFP: H/C, O/C molar ratio, and BET.

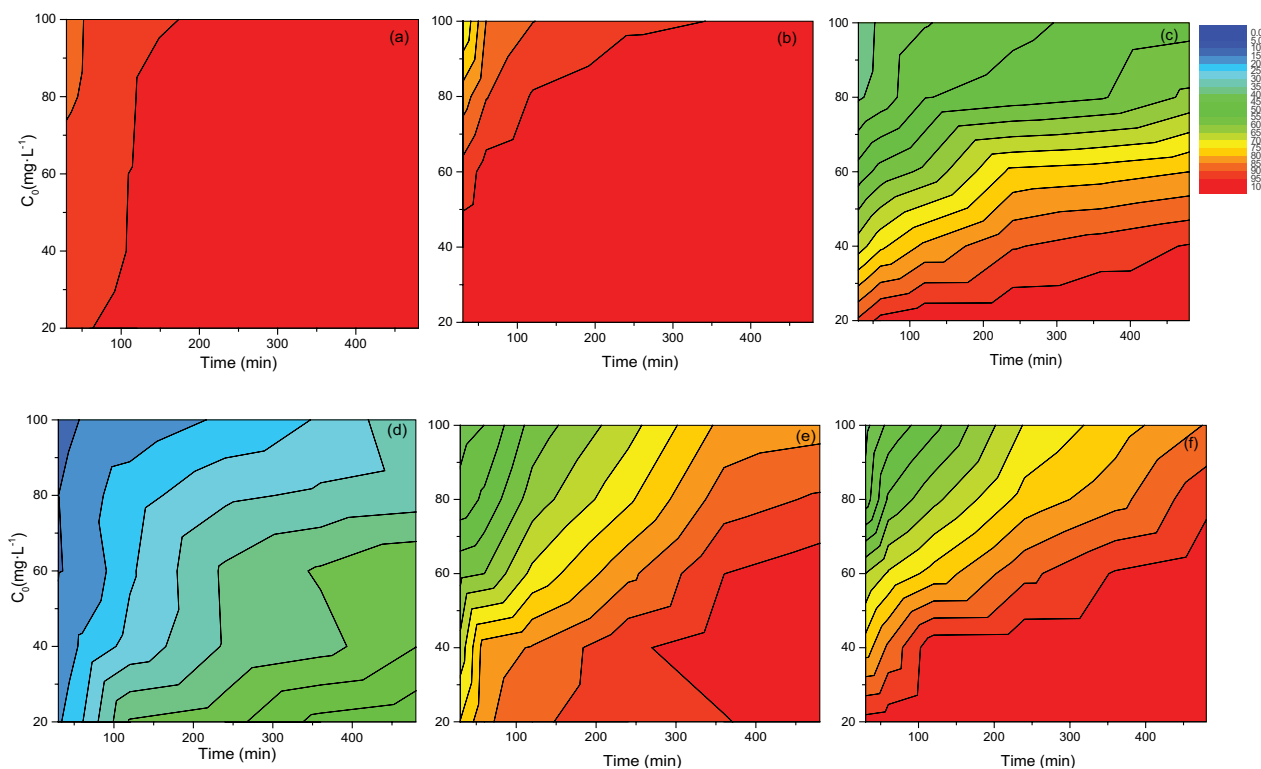


Fig. 7. Effect of solution concentration and adsorption time on the adsorption amount (25°C): (a) CMAD-MB, (b) CMSP-MB, (c) CMFP-MB, (d) CMAD-CR, (e) CMSP-CR, and (f) CMFP-CR.

of MB by CMSP slowly increases with the increase in time, especially at higher solution concentration. Nevertheless, the adsorption of MB by CMAD is close to equilibrium within 30 min, and it could quickly absorb MB even at a high concentration. Thus, the adsorption efficiency of CMAD is higher than that of CMSP. The CR adsorption performance of CMSP and CMFP is superior to that of CMAD. CR adsorption rate of CMFP is always faster than that of CMSP, and this performance is related to pore size. Biochar with large mesopores has less resistance to adsorbate [18]. The adsorption amount of CR by CMAD with a very small specific surface area is still very small even for a long time.

### 3.2.3. Effect of temperature on adsorption

The adsorption results at different temperatures are shown in Fig. 8. The MB adsorption amount does not change with the change in temperature under the low solution concentration, but the adsorption amount of MB increases with the rise in temperature when the solution concentration increases. The adsorption amount at 25°C is significantly lower than that at 45°C, which indicates that the adsorption process of MB by CMSP and CMFP is endothermic. The adsorption amount at high temperature is obviously better than that at low temperature under the same adsorption time condition. Therefore, the acting force between CMSP and CMFP and MB increases, the adsorption rate accelerates and the time for the reaction to reach equilibrium shortens with the increase in temperature. The adsorption amount of MB by CMAD firstly decreases and then increases as temperature increases, which means that the adsorption of CMAD is not a simple endothermic

or exothermic process. In the meantime, the rate of adsorption of CMAD also reduces firstly and then rises, which might be due to the dynamic balance of adsorption and desorption with temperature.

The CR adsorption amount of CMSP and CMFP increases under different solution concentrations as the adsorption temperature increases, which implies that the adsorption is an endothermic process. By contrast, the effect of temperature on the adsorption of CR by CMAD is not obvious. Comparing the adsorption of MB and CR by CMAD shows that temperature significantly affects the adsorption of MB.

### 3.3. Adsorption isotherm

Langmuir and Freundlich’s models are used to determine the adsorption type and limit [30,31]. Langmuir model describes that adsorption is a monolayer adsorption process [32], whilst the Freundlich model assumes that adsorption occurs on a multilayer heterogeneous surface [33].

Langmuir is as follows:

$$\frac{C_e}{q_e} = \frac{1}{q_{\max} B} + \frac{1}{q_{\max}} C_e \quad (3)$$

Freundlich is as follows:

$$\ln q_e = \ln K_f + \frac{1}{n} \ln C_e \quad (4)$$

where  $B$  is the Langmuir constant relevant to the adsorption energy ( $L \text{ mg}^{-1}$ );  $K_f$  is the Freundlich constant relevant to the

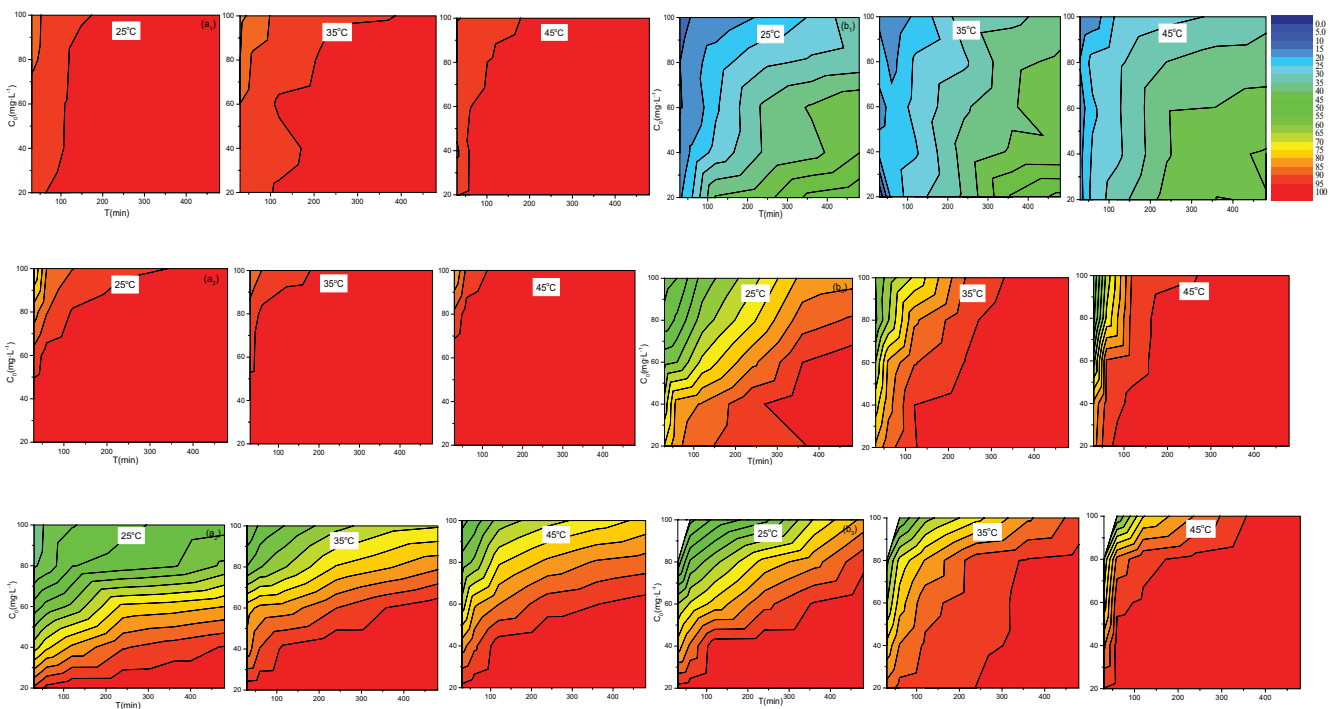


Fig. 8. Effect of temperature on adsorption of MB and CR by three adsorbents: (a<sub>1</sub> and b<sub>1</sub>) CMAD, (a<sub>2</sub> and b<sub>2</sub>) CMSP, (a<sub>3</sub> and b<sub>3</sub>) CMFP, where ‘a’ represents the adsorption diagram of MB and ‘b’ represents the adsorption diagram of CR.

adsorption performance of the adsorbent ( $L\ mg^{-1}$ );  $1/n$  is the adsorption intensity indicating the favourability of adsorption. The adsorption constants, adsorption capacity and correlation coefficients calculated through Langmuir and Freundlich models are shown in Table 2. The adsorption isothermal fitting curves at 25°C are shown in Fig. 9. Based on the value of  $R^2$ , adsorption of MB and CR by CMSP and CMFP conforms to Langmuir ( $R^2 > 0.99$ ). This relationship indicates that pores and oxygen-containing functional groups are evenly distributed on the surface of CMSP and CMFP, and the whole surface of CMSP and CMFP has the same adsorption capacity. The adsorption of MB and CR by CMAD is more consistent with Freundlich than Langmuir ( $R^2$ , 0.99 and 0.99 vs. 0.96 and 0.93), which means that adsorption is not limited to a monolayer, and MB amounts are adsorbed to the heterogeneous surface of CMAD [34]. The value of  $n$  is used to describe whether the adsorption is favourable. If  $n$  is between 1 and 2, then the adsorption process is favourable [35]. In this study, the value of  $n$  in the isotherm equation for adsorption of MB and CR by CMAD is greater than 1, which implies that CMAD has a good adsorption process.

### 3.4. Adsorption kinetics

The adsorption process of MB and CR on CMAD, CMSP and CMFP mainly shows two different stages. The first

stage is the rapid adsorption stage in the first few hours, and it is related to the functional groups and pores on the surface of adsorbent. The second stage is the slow adsorption stage, in which most of the active sites on the adsorbent are occupied [36]. The adsorptions of CR on CMSP and CMFP reach a slow adsorption process at 360 and 480 min, respectively. Similarly, the adsorptions of MB on CMSP, CMFP and CMAD reach a slow adsorption process at 240, 360 and 120 min, respectively. Therefore, the influence of oxygen-containing functional groups on the adsorption rate is greater than that of pores. The adsorption rate of CMAD to MB is faster than that of CMSP and CMFP because the former has a higher content of oxygen-containing functional groups.

The pseudo-first-order model and pseudo-second-order model are used to study the adsorption kinetic [11,33].

$$\log(q_e - q_t) = \log q_e - \frac{k_1}{2.303} t \quad (5)$$

$$\frac{t}{q_i} = \frac{1}{k_2 q_e^2} + \frac{t}{q_e} \quad (6)$$

where  $k_1$  ( $h^{-1}$ ) and  $k_2$  ( $g\ mg^{-1}\ h^{-1}$ ) are the rate constants of the pseudo-first-order model and pseudo-second-order

Table 2  
Langmuir and Freundlich constants and correlation coefficients

Absorbate	Sample	Langmuir			Freundlich		
		$q_{max}$ ( $mg\ g^{-1}$ )	$B$ ( $mg\ g^{-1}$ )	$R^2$	$K_F$ ( $L\ mg^{-1}$ )	$1/n$	$R^2$
MB	CMAD	81.23	0.25	0.96	15.55	0.74	0.99
	CMSP	39.68	7.16	0.99	29.58	0.28	0.86
	CMFP	21.14	1.34	0.99	14.53	0.098	0.95
CR	CMAD	21.10	0.03	0.93	1.175	0.59	0.99
	CMSP	34.69	2.64	0.99	21.25	0.19	0.89
	CMFP	34.87	1.17	0.99	21.25	0.19	0.89

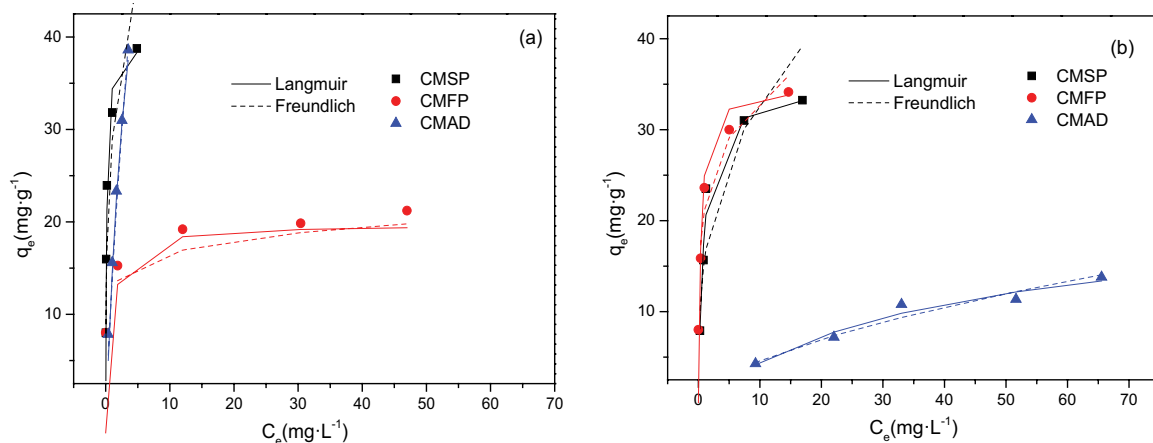


Fig. 9. Isotherms of organic matter adsorption on samples: (a) MB and (b) CR ( $C_0 = 100\ mg\ L^{-1}$ ;  $T = 25^\circ C$ ).

Table 3  
 Constants and correlation coefficients of pseudo-first-order and pseudo-second-order models

Absorbate	Sample	Pseudo-first-order model				Pseudo-second-order model		
		$q_{e,exp}$	$q_{e,cal}$	$k_1$	$R^2$	$q_{e,cal}$	$k_2$	$R^2$
		( $\text{mg g}^{-1}$ )	( $\text{mg g}^{-1}$ )			( $\text{mg g}^{-1}$ )		
MB	CMAD	38.60	4.16	0.011	0.92	38.88	0.00695	0.99
	CMSP	38.75	8.93	0.0078	0.89	39.54	0.0022	0.99
	CMFP	21.21	7.96	0.0071	0.98	21.95	0.0021	0.99
CR	CMAD	13.79	8.83	0.0026	0.97	14.57	0.00074	0.92
	CMSP	33.24	28.44	0.0094	0.85	36.95	0.00045	0.99
	CMFP	34.16	22.47	0.0054	0.99	37.64	0.00039	0.99

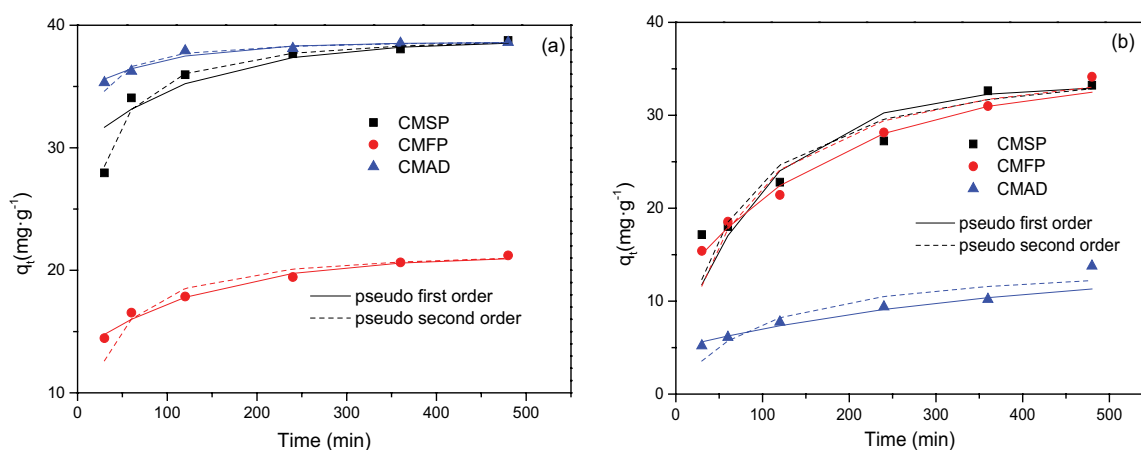


Fig. 10. Adsorption kinetics of organic matter adsorption on CMAD, CMSP and CMFP: (a) MB and (b) CR.

model, respectively. The results are shown in Fig. 10 and Table 3. As shown in Table 3, the value of  $q_e$  determined by experiments is very close to the value calculated by the pseudo-second-order model. According to  $R^2$ , the adsorption of MB and CR by CMSP conforms to the pseudo-second-order equation ( $R^2 > 0.99$ ). The adsorption of MB by CMFP conforms to the pseudo-second-order equation, whilst the adsorption of CR conforms to the two models. The adsorption of MB by CMAD conforms to the pseudo-second-order model, whilst the adsorption of CR conforms to the pseudo-first-order model. The pseudo-first-order equation is based on the physical process of adsorption. The pseudo-second-order model indicates that the affecting factor of adsorption is chemisorption [37]. The MB adsorption mechanism of CMAD is more accurate than the pseudo-first-order model. This finding indicates that the adsorption of MB by three adsorbents is mainly chemical adsorption. For CR with larger molecular size, the adsorption of CR by CMSP is a chemical action, whilst the adsorption of CR by CMFP and CMAD is a physical action.

#### 4. Conclusions

This study prepared CMAD at biochemical treatment and CMSP and CMFP at thermal chemical treatment.

The structural characteristics and adsorption properties of the three samples were compared. The results show that CMAD has a very small specific surface area, but it has abundant surface functional groups. As a result, it has an excellent adsorption performance for alkaline organic matter and can be used as a potential adsorbent. The adsorptions of MB on CMSP, CMFP and CMAD reach a slow adsorption process at 240, 360 and 120 min, respectively. Even though CMAD has a low degree of graphitisation and a weak structural stability, it can adsorb organics very quickly and can be used as an adsorbent. The maximum removal rates by CMSP, CMFP and CMAD are 96.88%, 53.03% and 95.72% for MB, respectively. The strong adsorption capacity of MB by CMAD is related to its rich functional groups on the surface, and the weak adsorption capacity of CR is related to its extremely low specific surface area. Biochar with excellent adsorption performance should have the following distinct characteristics: high stability, such as high fixed carbon content, and large specific surface area and rich oxygen-containing functional groups, such as CMSP. The specific surface area of CMAD can be enlarged by pyrolysis. In the meantime, the pyrolysis conditions should be controlled to prevent the decomposition of functional groups. The physical or chemical modification can also be used to promote the development of the specific surface area without reducing the functional groups.

## Acknowledgments

This research was financially supported by the Fundamental Research Funds for the Central Universities (2662019PY018, 201810504073), and the Major Projects of Technical Innovation of Hubei Province (2019ACA153). The authors also acknowledge the extended help from the Analytical and Testing Center of Huazhong Agricultural University (HZAU).

## References

- M.J. Ahmed, P.U. Okoye, E.H. Hummadi, B.H. Hameed, High-performance porous biochar from the pyrolysis of natural and renewable seaweed (*Gelidium acerosa*) and its application for the adsorption of methylene blue, *Bioresour. Technol.*, 278 (2019) 159–164.
- M. Stefaniuk, P. Bartmiński, K. Różyło, R. Dębicki, P. Oleszczuk, Ecotoxicological assessment of residues from different biogas production plants used as fertilizer for soil, *J. Hazard. Mater.*, 298 (2015) 195–202.
- N.-m. Zhu, T. Luo, X.-j. Guo, H. Zhang, Y. Deng, Nutrition potential of biogas residues as organic fertilizer regarding the speciation and leachability of inorganic metal elements, *Environ. Technol.*, 36 (2015) 992–1000.
- S. Menardo, F. Gioelli, P. Balsari, The methane yield of digestate: effect of organic loading rate, hydraulic retention time, and plant feeding, *Bioresour. Technol.*, 102 (2010) 2348–2351.
- Z. Tang, Y.F. Deng, T. Luo, Y.-s. Xu, N.-m. Zhu, Enhanced removal of Pb(II) by supported nanoscale Ni/Fe on hydrochar derived from biogas residues, *Chem. Eng. J.*, 292 (2016) 224–232.
- M. Stefaniuk, P. Oleszczuk, Characterization of biochars produced from residues from biogas production, *J. Anal. Appl. Pyrolysis*, 115 (2015) 157–165.
- S.-H. Ho, Y.-d. Chen, Z.-k. Yang, D. Nagarajan, J.-S. Chang, N.-q. Ren, High-efficiency removal of lead from wastewater by biochar derived from anaerobic digestion sludge, *Bioresour. Technol.*, 246 (2017) 142–149.
- A. Çelekli, B. Bozkuş, H. Bozkurt, Development of a new adsorbent from pumpkin husk by KOH-modification to remove copper ions, *Environ. Sci. Pollut. Res.*, 26 (2019) 11514–11523.
- Y. Zhu, B.J. Yi, Q.X. Yuan, Y.L. Wu, M. Wang, S.P. Yan, Removal of methylene blue from aqueous solution by cattle manure-derived low temperature biochar, *RSC Adv.*, 8 (2018) 19917–19929.
- R.K.V. Giri, L.S. Raju, Y.V. Nancharaiiah, M. Pulimi, N. Chandrasekaran, A. Mukherjee, Anaerobic nano zero-valent iron granules for hexavalent chromium removal from aqueous solution, *Environ. Technol. Innovation*, 16 (2019) 100495, doi: 10.1016/j.eti.2019.100495.
- S.V. Manjunath, R.S. Baghel, M. Kumar, Performance evaluation of cement–carbon composite for adsorptive removal of acidic and basic dyes from single and multi-component systems, *Environ. Technol. Innovation*, 16 (2019) 100478, doi: 10.1016/j.eti.2019.100478.
- M.A. Al-Ghouti, A.O. Sweleh, Optimizing textile dye removal by activated carbon prepared from olive stones, *Environ. Technol. Innovation*, 16 (2019) 100488, doi: 10.1016/j.eti.2019.100488.
- Z.H. Ding, X.B. Xu, T. Phan, X. Hu, G.Z. Nie, High adsorption performance for As(III) and As(V) onto novel aluminum-enriched biochar derived from abandoned Tetra Paks, *Chemosphere*, 208 (2018) 800–807.
- H. Lachheb, E. Puzenat, A. Houas, M. Ksibi, E. Elaloui, C. Guillard, J.-M. Herrmann, Photocatalytic degradation of various types of dyes (Alizarin S, Crocein Orange G, Methylene Red, Congo Red, Methylene Blue) in water by UV-irradiated titania, *Appl. Catal.*, B, 39 (2002) 75–90.
- K.-M. Poo, E.-B. Son, J.-S. Chang, X.H. Ren, Y.-J. Choi, K.-J. Chae, Biochars derived from wasted marine macro-algae (*Saccharina japonica* and *Sargassum fusiforme*) and their potential for heavy metal removal in aqueous solution, *J. Environ. Manage.*, 206 (2018) 364–372.
- J. Shang, J.C. Pi, M.Z. Zong, Y.R. Wang, W.H. Li, Q.H. Liao, Chromium removal using magnetic biochar derived from herb-residue, *J. Taiwan Inst. Chem. Eng.*, 68 (2016) 289–294.
- B.L. Chen, Z.M. Chen, S.F. Lv, A novel magnetic biochar efficiently sorbs organic pollutants and phosphate, *Bioresour. Technol.*, 102 (2011) 716–723.
- S.R. Sandeman, V.M. Gun'ko, O.M. Bakalinska, C.A. Howell, Y.S. Zheng, M.T. Kartel, G.J. Phillips, S.V. Mikhalovsky, Adsorption of anionic and cationic dyes by activated carbons, PVA hydrogels, and PVA/AC composite, *J. Colloid Interface Sci.*, 358 (2011) 582–592.
- X.M. Peng, F.P. Hu, T. Zhang, F.X. Qiu, H.L. Dai, Amine-functionalized magnetic bamboo-based activated carbon adsorptive removal of ciprofloxacin and norfloxacin: a batch and fixed-bed column study, *Bioresour. Technol.*, 249 (2017) 924–934.
- M.E. Parolo, M.C. Savini, R.M. Loewy, Characterization of soil organic matter by FT-IR spectroscopy and its relationship with chlorpyrifos sorption, *J. Environ. Manage.*, 196 (2017) 316–322.
- M. Jouiad, N. Al-Nofeli, N. Khalifa, F. Benyettou, L.F. Yousef, Characteristics of slow pyrolysis biochars produced from rhodes grass and fronds of edible date palm, *J. Anal. Appl. Pyrolysis*, 111 (2015) 183–190.
- M. Essandoh, D. Wolgemuth, C.U. Pittman Jr., D. Mohan, T. Mlsna, Phenoxo herbicide removal from aqueous solutions using fast pyrolysis switchgrass biochar, *Chemosphere*, 174 (2017) 49–57.
- A.Q. Yang, G.M. Zhang, G. Yang, H.Y. Wang, F. Meng, H.C. Wang, M. Peng, Denitrification of aging biogas slurry from livestock farm by photosynthetic bacteria, *Bioresour. Technol.*, 232 (2017) 408–411.
- D. González, M.A. Montes-Morán, A.B. Garcia, Influence of inherent coal mineral matter on the structural characteristics of graphite materials prepared from anthracites, *Energy Fuels*, 19 (2005) 263–269.
- M. Einert, C. Wessel, F. Badaczewski, T. Leichtweiß, C. Eufinger, J. Janek, J. Yuan, M. Antonietti, B.M. Smarsly, Nitrogen-doped carbon electrodes: influence of microstructure and nitrogen configuration on the electrical conductivity of carbonized polyacrylonitrile and poly(ionic liquid) blends, *Macromol. Chem. Phys.*, 216 (2015) 1930–1944.
- H.-M. Cheng, H. Endo, T. Okabe, K. Saito, G.-B. Zheng, Graphitization behavior of wood ceramics and bamboo ceramics as determined by X-ray diffraction, *J. Porous Mater.*, 6 (1999) 233–237.
- Z.H. Ding, X. Hu, Y.S. Wan, S.S. Wang, B. Gao, Removal of lead, copper, cadmium, zinc, and nickel from aqueous solutions by alkali-modified biochar: batch and column tests, *J. Ind. Eng. Chem.*, 33 (2016) 239–245.
- X.D. Cao, W. Harris, Properties of dairy-manure-derived biochar pertinent to its potential use in remediation, *Bioresour. Technol.*, 101 (2010) 5222–5228.
- J. Li, D.H.L. Ng, P. Song, C. Kong, Y. Song, P. Yang, Preparation and characterization of high-surface-area activated carbon fibers from silkworm cocoon waste for congo red adsorption, *Biomass Bioenergy*, 75 (2015) 189–200.
- S.V. Novais, M.D.O. Zenero, J. Tronto, R.F. Conz, C.E.P. Cerri, Poultry manure and sugarcane straw biochars modified with MgCl<sub>2</sub> for phosphorus adsorption, *J. Environ. Manage.*, 214 (2018) 36–44.
- D. Gümüş, F. Gümüş, The use of a wetland plant as a new biosorbent for treatment of water contaminated with heavy metals: nonlinear analyses, modification, competitive effects, *Environ. Technol. Innovation*, 16 (2019) 100483, doi: 10.1016/j.eti.2019.100483.
- S. Jamil, P. Loganathan, J. Kandasamy, A. Listowski, C. Khourshed, R. Naidu, S. Vigneswaran, Removal of dissolved organic matter fractions from reverse osmosis concentrate: comparing granular activated carbon and ion exchange resin adsorbents, *J. Environ. Chem. Eng.*, 7 (2019) 103126, doi: 10.1016/j.jece.2019.103126.
- T.L. Silva, A. Ronix, O. Pezoti, L.S. Souza, P.K.T. Leandro, K.C. Bedin, K.K. Beltrame, A.L. Cazetta, V.C. Almeida,

- Mesoporous activated carbon from industrial laundry sewage sludge: adsorption studies of reactive dye Remazol Brilliant Blue R, *Chem. Eng. J.*, 303 (2016) 467–476.
- [34] D. Xia, F. Tan, C.P. Zhang, X.L. Jiang, Z. Chen, H. Li, Y.M. Zheng, Q.B. Li, Y.P. Wang, ZnCl<sub>2</sub>-activated biochar from biogas residue facilitates aqueous As(III) removal, *Appl. Surf. Sci.*, 377 (2016) 361–369.
- [35] J.-H. Park, Y.S. Ok, S.-H. Kim, J.-S. Cho, J.-S. Heo, R.D. Delaune, D.-C. Seo, Competitive adsorption of heavy metals onto sesame straw biochar in aqueous solutions, *Chemosphere*, 142 (2016) 77–83.
- [36] G. Yang, L. Wu, Q.M. Xian, F. Shen, J. Wu, Y.Z. Zhang, Removal of congo red and methylene blue from aqueous solutions by vermicompost-derived biochars, *PLoS One*, 11 (2016) e0154562, doi: 10.1371/journal.pone.0154562.
- [37] K. Björklund, L.Y. Li, Adsorption of organic stormwater pollutants onto activated carbon from sewage sludge, *J. Environ. Manage.*, 197 (2017) 490–497.